Detailed magnetization study of $NdCu_2$ at low temperatures

1995 J. Phys.: Condens. Matter 7 1897

(http://iopscience.iop.org/0953-8984/7/9/014)

J. Phys.: Condens. Matter 7 (1995) 1897–1907. Printed in the UK

Detailed magnetization study of $NdCu_2$ at low temperatures

M Ellerby†, K A McEwen†, M de Podesta†, M Rotter‡ and E Gratz‡

† Department of Physics, Birkbeck College, University of London, London, WC1E 7HX, UK

‡ Institut für Experimentalphysik, Technische Universität Wien, A-1040 Wien, Austria

Received 15 November 1994

Abstract. The magnetization of $NdCu_2$ has been measured from 0.3 to 7.0 K, in fields up to 12 T. The correspondence of the magnetization with a zero-field neutron diffraction study is considered. A model is proposed in order to explain the various magnetic phases observed in the magnetization data.

1. Introduction

$RECu_2$ compounds exhibit a variety of magnetic structures. These compounds all crystallize in the orthorhombic (IMMA) $CeCu_2$-type structure; $LaCu_2$ being the exception, crystallizing in a hexagonal AlB_2-type structure. This isomorphism allows for a comprehensive study of the interplay between the crystal-field, magnetoelastic and exchange energies.

There have been several recent studies on polycrystalline $NdCu_2$ [1, 2, 3] clarifying the lattice parameters, determining the crystal-field parameters and the importance of the crystal field in the behaviour of $NdCu_2$. These studies also considered the transport properties in polycrystalline material.

There has only been one study of a single-crystal sample, by Svoboda *et al* [4]. This study reported magnetoresistance and magnetization measurements for the b-axis, and summarised the results in a phase diagram. From these results they concluded that in zero field there are four antiferromagnetic phases, with $T_N = 6.5$ K.

A recent neutron diffraction study performed by Arons *et al* [5] on polycrystalline material found the following features for $NdCu_2$. The moments are constrained to the b–c plane and are ordered ferromagnetically along the b-axis. Between 1.4 K and $T_N = 6.5$ K, they found two principal structures with a modulation vector parallel to the a-axis. Between T_N and $T = 4$ K they found the structure to be incommensurate, with an ordering wave vector $q_0 = (0.6135,\ 0.042,\ 0)$. Below this temperature they found the structure to be commensurate. At $T = 1.4$ K first- and third-harmonic satellites were observed with an associated wave vector $q = (0.6,\ 0,\ 0)$. The moments associated with these satellites were 2.32 μ_B and 0.9 μ_B respectively. This gave an average moment of 1.72 μ_B/Nd atom in the magnetic cell composed of five crystallographic unit cells. Between the incommensurate and commensurate phases an additional state was observed. This state was successfully modelled using a superposition of patterns derived from the two ordering wave vectors q_0 and q. In addition, the observation of the third harmonic in this intermediate phase supports the interpretation that this state may be described as a mixture of the commensurate low-temperature and the incommensurate high-temperature phases. Thus they [5] conclude that there are only two magnetic spin configurations present below T_N for zero field. This does not accord with the result found in the single crystal previously examined [4].

0953-8984/95/091897+11$19.50

Our new study, performed on a single crystal, extends the work [1, 4] to higher fields and lower temperatures, producing data of higher precision.

2. Experimental details

A single crystal of $NdCu_2$ was grown using the Czochralski method. The dimensions of the sample used were approximately $3 \times 3 \times 2.6$ mm ($m = 0.1844$ g). This study was made in the temperature range $T = 0.3$–7.0 K for fields up to 12 T. The measurements were made at Birkbeck College, using a vibrating-sample magnetometer (VSM) operating in conjunction with a top-loading ^{3}He cryostat, constructed by Oxford Instruments plc.

The sample was mounted in the VSM with the b-axis parallel to the applied field. In this orientation, magnetization measurements were made as a function of temperature by heating in a constant field, and as a function of applied field at constant temperature. Before each isothermal magnetization measurement, the sample was heated above T_N(annealed) and cooled to the required temperature in zero field.

The cryostat is operated with the sample immersed in liquid ^{3}He for the temperature range $T = 0.3$–1.5 K. For $T > 1.5$ K the sample is cooled using the ^{3}He as an exchange gas with the 1 K ^{4}He bath providing the heat sink. Temperature control is achieved using a Speer resistance thermometer for $T \leqslant 4.2$ K, and a carbon-glass resistance thermometer for temperatures above this. Since no thermometer may be placed in close proximity to the vibrating sample, there exists some uncertainty in its temperature. In order to overcome this uncertainty, the temperature control for this cryostat incorporates three interdependent control regions to provide the correct temperature profile within the cryostat.

3. Results

In this section we outline the principal features of the magnetization measurements presented in figures 1–3.

In figure 1 we see at $T = 7.0$ K ($> T_N$) the response is that of a paramagnetic material. On reducing the temperature to 5.0 K a transition appears at $B = 2.3$ T. We define the transition field as the midpoint of magnetization change (maximum of dM/dB). At $T = 4.0$ K two further transitions appear at $B = 0.5$ T and a very weak transition at $B = 1.3$ T. In addition the upper transition has become much sharper and moved to $B = 2.6$ T. For $T = 3.3$ K we see that the low-field behaviour has become more complex, with three transitions occurring between $B = 0.7$ and 1.0 T. At higher fields there is an extra transition at $B = 2.3$ T. At this temperature the hysteresis is clear on all transitions and quite small in magnitude. The magnetization data at $T = 2.00$ K shows fewer field-induced transitions, all of which show first-order behaviour with hysteresis at each transition. The transitions observed at $B = 0.75$ and 2.75 T for $T = 2.00$ K were also reported by [2, 4]. In these earlier magnetization studies the transitions were not as sharp. In addition the transition observed at $B = 2.6$ T ($T = 2.00$ K) was not observed in the study by Svoboda *et al* [4] whilst it was detected by Zochowski *et al* [10].

There are subtle changes in the magnetization between $T = 0.33$ and 1.62 K, as shown in figure 2. For $T = 1.62$ K three distinct transitions for increasing and decreasing fields were observed. At $T = 1.00$ K there are three transitions for field increasing, whilst there are four in decreasing field. For $T = 0.50$ K this overall behaviour was fully established. However, on reducing the temperature to $T = 0.33$ K the response to decreasing field was modified, leaving only one extra transition.

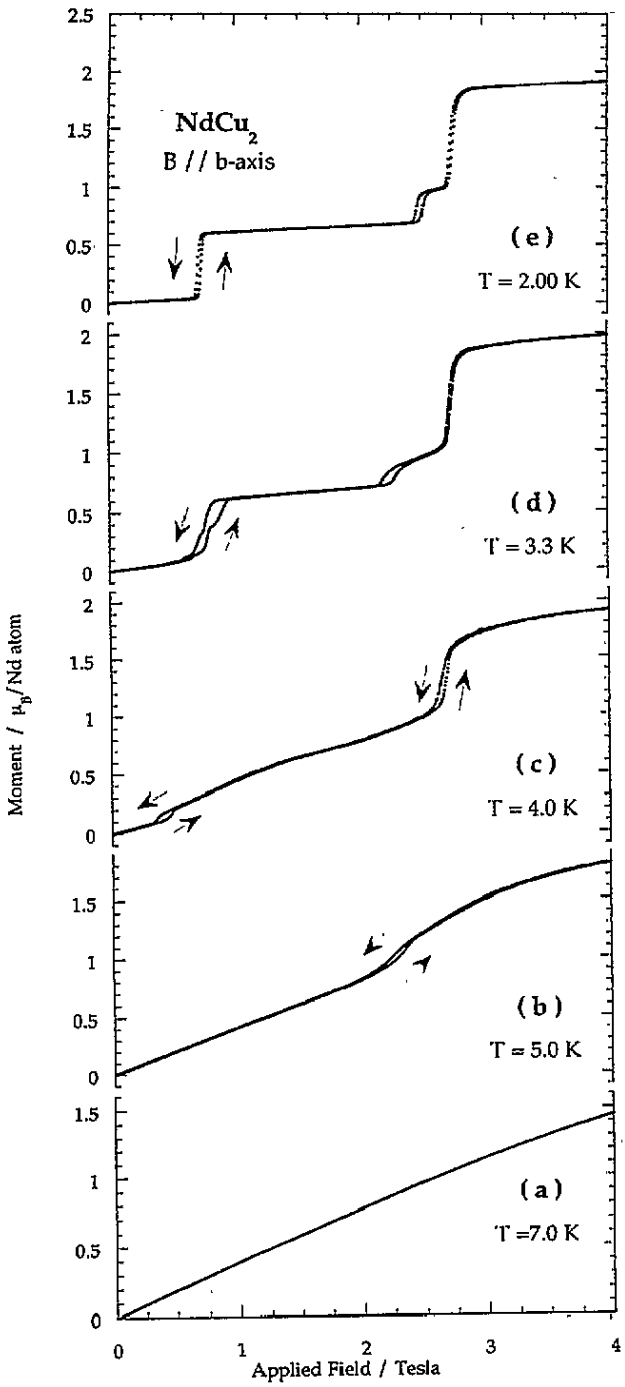

Figure 1. Magnetization measurements for temperatures in the range $T = 0.3$–7.0 K, in fields up to $B = 4$ T parallel to the b-axis. Where hysteresis is present, arrows indicate the direction in which the applied field is being ramped.

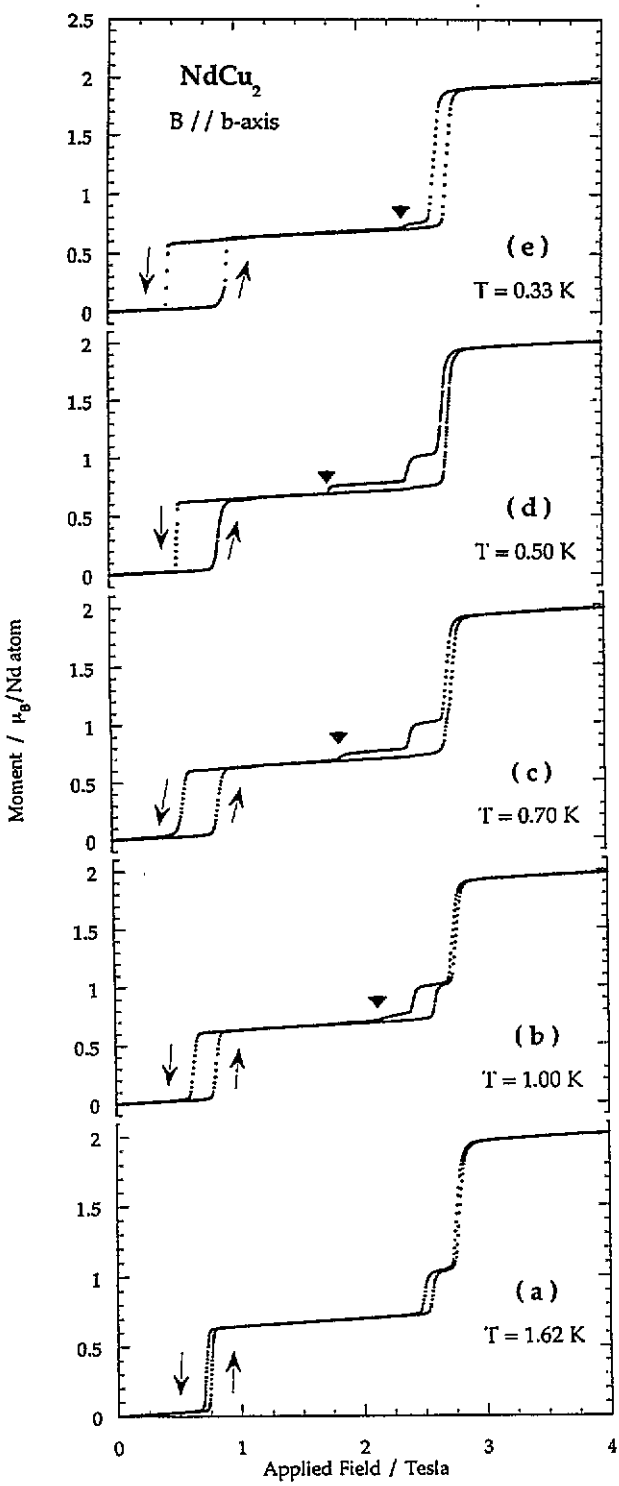

Figure 2. The magnetization between $T = 0.33$ and 1.62 K showing the development of the additional transitions observed in decreasing field.

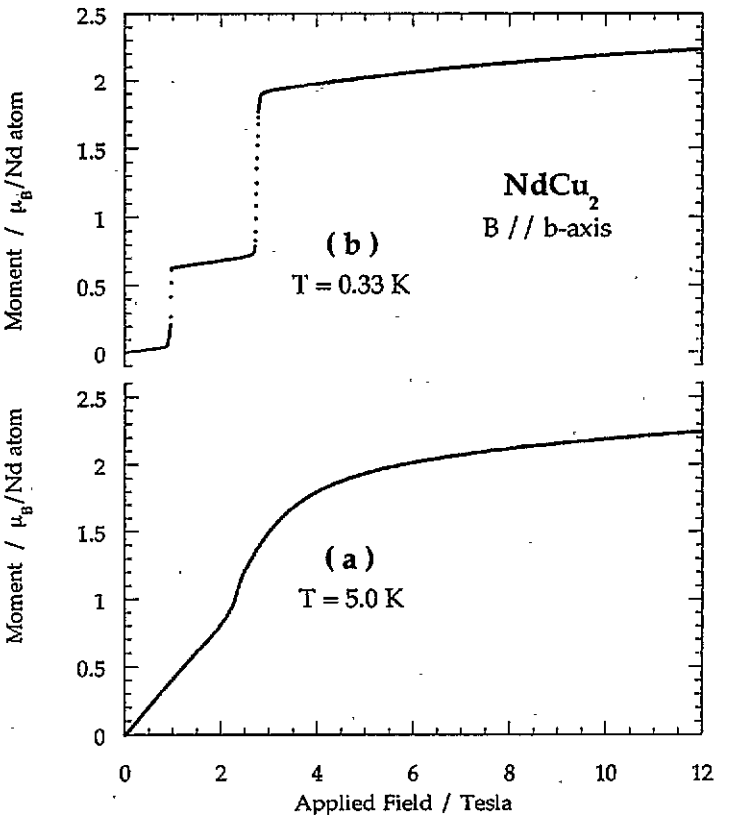

Figure 3. Magnetization measurements in fields up to $B = 12$ T at (a) 5.0 K and (b) 0.33 K. Data for increasing fields only are shown here.

Comparing the results for $T = 1.62$ and 0.50 K (figure 2 (a) and (d)) there are several clear distinctions. For increasing fields there are three transitions at $T = 1.62$ K. These transitions occur at $B = 0.75$, 2.6 and 2.75 T, with moments after the transitions of 0.62, 1.04 and 1.94 μ_B respectively. On increasing the field at $T = 0.50$ K there are only two transitions occurring at $B = 0.9$ and 2.75 T, with moments of 0.61 and 1.94 μ_B respectively. This behaviour is also present if the sample is not annealed before increasing the field. However, the transition at $B = 0.9$ T becomes sharper in this case.

For decreasing fields the behaviour becomes more complex. At $T = 0.50$ K, four transitions are then observed. These occur at 2.7, 2.4, 1.8 and 0.55 T, with associated moments after the transitions of 1.02, 0.75, 0.61 and 0.03 μ_B. The phase between $B = 2.7$ and 2.4 T in decreasing fields at $T = 0.50$ K may be associated with the phase between $B = 2.75$ and 2.5 T for $T = 1.62$ K, since the moments are of a similar magnitude. However, the phase observed between $B = 2.4$–1.8 T for $T = 0.50$ K has no correspondence with the measurement at $T = 1.62$ K.

Figure 3 shows two magnetization measurements performed up to $B = 12$ T. Neither of these results showed evidence of transitions above $B = 4$ T. The moment at 12 T and $T = 0.33$ K is 2.25 ± 0.05 μ_B. This is to be contrasted with the moment determined by extrapolation back to $B = 0$ which is 1.74 ± 0.04 μ_B, showing that there is some moment induced by the field.

4. Discussion and analysis

The value of 1.72 μ_B/Nd atom deduced from neutron powder diffraction measurements [5] gives the magnitude of the sublattice moment, in zero field, of the antiferromagnetic structure shown in figure 4. The moment determined by linear extrapolation of the magnetization at $T = 0.33$ K from the saturation value is 1.74 μ_B/Nd atom. This value indicates that the primary magnetization process is one of a sequence of spin flips. Figure 3(a) shows the magnetization in the incommensurate-phase region at 5 K. In contrast to the spin-flip transitions at low temperatures, there is a linear increase at low fields followed by a progressive saturation in the ferromagnetic state. This smooth behaviour is closely connected with the incommensurate nature of this region in the magnetic phase diagram, where the modulation is nearly sinusoidal. The Néel temperature determined from the temperature derivative of the magnetization, in $B = 0.1$ T, was found to be $T_N = 6.7$ K. This is slightly higher than that observed in other studies [4, 5].

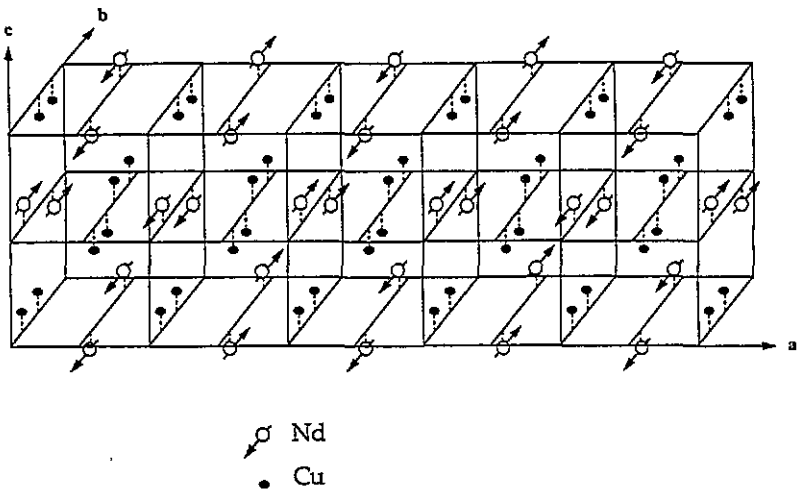

Figure 4. Spin arrangement in the magnetic unit cell of $NdCu_2$ in zero field for $T < 4$ K [5, 6].

We see in figure 4 the spin structure within the magnetic unit cell for $NdCu_2$ in zero field with $T < 4$ K [5, 6]. The arrows indicate the orientation of the Nd moments relative to the *b*-axis. In this figure we note that the Nd moments are ordered ferromagnetically within the *b*–*c* planes, pointing in the *b*-direction: these planes are antiferromagnetically ordered with the modulation parallel to the *a*-axis. The magnetic unit cell is five crystallographic unit cells long. We note the different alignment of the moments in the two right-hand crystallographic units.

From the measurements described in section 3 we expect that the magnetization in $NdCu_2$ may be accounted for by a sequence of spin flips. Figure 5 depicts the spin-flip structures, for $T = 0$ K, as concluded from very recently performed neutron diffraction experiments on a single crystal in a magnetic field [7]. The arrows in the figure represent the alignment of moments in the *b*–*c* plane. The squares enclosing each pair of arrows are intended to denote the crystallographic unit cell, and thus giving an equivalent of four Nd^{3+} ions.

In order to understand the behaviour of the various field-induced spin configurations observed for increasing fields, we adopt and modify a model proposed by Gignoux *et al* [8] in their study of $CeZn_2$. $CeZn_2$ also exhibits a strong uniaxial anisotropy, though the

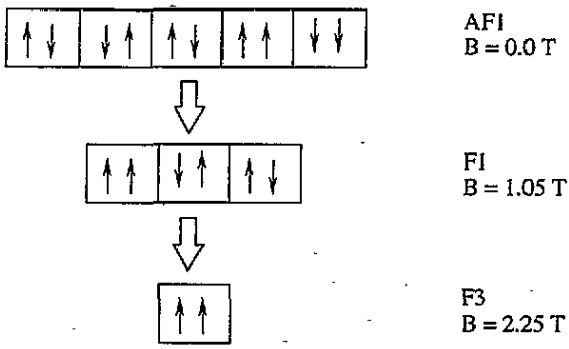

Figure 5. Structures determined at $T = 0$ K using the model described in the text. Calculated transition fields are given. The labels AFI, FI and F3 denote the antiferromagnetic, ferrimagnetic and ferromagnetic phases [7]. The arrows within each box represent the directions of the moments at $(0,\ 1/2 \pm y,\ 0 \pm z)$ and $(1/2,\ 1/2 \pm y,\ 1/2 \mp z)$ [1] for each of the cells, where $y = 0.25$ and $z = 0.4617$.

magnetic structure is somewhat different.

We now outline the basic assumptions of our effective $S = 1/2$ model and then construct the Hamiltonian and describe the appropriate constraints.

(i) Two-site fluctuations have been neglected using a mean-field theory [9]

(ii) The properties of the ordered state are governed by a crystal-field Kramers doublet ground state with a huge uniaxial magnetic anisotropy in the b-direction, thus producing an Ising-like behaviour

(iii) All the moments in one b–c plane order ferromagnetically, with the b-axis being the easy axis.

To describe the properties of the ordered state we use a Heisenberg Hamiltonian of the type given in (1),

$$H_{\mathrm{mag}} = -\frac{1}{2}\sum_{i,j} n(i\text{–}j) M_i \cdot M_j - \sum_i M_i \cdot H \tag{1}$$

where $M_i = g_J \mu_B J_i$ represents the magnetic moment of one ion in the ith b–c plane and $n(i\text{–}j)$ denotes the coupling between planes i and j. This Hamiltonian already assumes that all moments in a b–c plane are equal. In a mean-field theory, the molecular field which the ions of the jth b–c plane produce at any ion of the ith b–c plane is then $n(i\text{–}j)\langle M_j\rangle$. At zero temperature all moments will saturate: $\langle M_i\rangle = \pm M_0$, the sign depending on the position of the moment in the magnetic unit cell, where M_0 is the saturation moment of the crystal-field ground state doublet and the magnetic free energy per ion for a given spin arrangement $\langle M_i\rangle$ can be written in the form

$$f(H) = \frac{F - F_0}{N} = -\frac{1}{2}\sum_{i,j} n(i\text{–}j)\frac{\langle M_i\rangle\langle M_j\rangle}{N} - \sum_i \frac{\langle M_i\rangle H}{N} \tag{2}$$

where N denotes the number of b–c planes in the crystal. This expression can be evaluated for the different possible spin arrangements, designated as AFI, FI and F3 in figure 5, consistent with results for increasing field at $T = 0.33$ K. Two equations for the coupling parameters $n(i\text{–}j)$ can be deduced from the critical fields $H_{c1}(\mathrm{AFI} \rightarrow \mathrm{FI})$ and $H_{c2}(\mathrm{FI} \rightarrow \mathrm{F3})$ (see, e.g., [8])

$$f_{\mathrm{AFI}}(H_{c1}) = f_{\mathrm{FI}}(H_{c1}) \tag{3}$$

$$f_{F1}(H_{c2}) = f_{F3}(H_{c2}). \tag{4}$$

According to the Landau expansion for the free energy a third condition is imposed by the ordering temperature T_N

$$kT_N = M_0^2 \sum_{m=-\infty}^{\infty} n(m)e^{-imq_0 \cdot a} \tag{5}$$

where $q_0 = 0.6135a^*$ is the incommensurate wavevector of the ordered phase near T_N and a is the lattice vector in the a-direction. Just below T_N the q_0-phase will be stable if the Fourier transform of the coupling constants $n(q) = \sum_{m=-\infty}^{\infty} n(m)e^{-imq \cdot a}$ has its maximum value at $q = q_0$ (see, e.g., [9]) imposing the condition

$$\nabla n(q)|_{q=q_0} = 0 \tag{6}$$

onto the coupling parameters.

We have considered interactions up to the seventh-nearest neighbour $n(j = 0, \ldots, 7)$. In this case we have to make appropriate assumptions for four of those parameters: the other four are determined by the conditions mentioned above (equations (3)–(6)). A set of possible values for the $n(j)$ is given in table 1. Knowledge of the actual values of the coupling parameters would enable us to calculate the spin dynamics.

Table 1. Mean field parameters, $n(i-j)$, determined from equations (3)–(6).

$i-j$	0	1	2	3	4	5	6	7
$n(i-j)M_0$ (T)	2.193	−0.894	−0.170	0.105	−0.036	−0.425	0.213	0.275

At finite temperatures the free energy f was calculated for the different possible spin arrangments using a self-consistent mean-field approach. The saturation moment for the calculation has been chosen to be $M_0 = 2.1\ \mu_B$ to be in agreement with the moments observed in each phase. The incommensurate phase was modelled using a magnetic unit cell with 100 b–c planes. A search was made, at a certain point (B, T), for the structure with the lowest free energy. It is for this structure that the moment has been calculated.

Figure 6 shows the comparison of isothermal magnetization measurements at 2.0 and 4.0 K with magnetization curves calculated using the parameters in table 1 (solid line). We see that at 4.0 K the agreement is strikingly close for the behaviour below about 2 T, but the position of the ferromagnetic transition is not precisely modelled. This may be due to the neglect of two-site fluctuations in the mean-field model. For 2.0 K we observe that the model predicts only two transitions.

Figure 7(a) is the phase diagram determined by our magnetization measurements. The different symbols indicate measurements at constant temperature (open circle) and constant field (filled circle). The lines serve as a guide to the eyes. The various regions of the phase diagram have been marked in accord with the structures determined by the model. The incommensurate phase is denoted by INC. The shaded region between the two phases AF1 and F1 indicates the width of the hysteresis observed in the magnetization. In this figure we have omitted the complex behaviour from F3 towards F1 below 1.6 K (see figure 2).

In the model calculation the (B, T) region of the phase diagram was calculated with steps of 0.1 T and 0.5 K. From this calculation phase boundaries have been derived and are indicated by solid lines in figure 7(b). The overall agreement with the experimental results is quite good and in particular, the phase AF1 is well reproduced. The model predicts a number of different long-period incommensurate stuctures all having similar free energies.

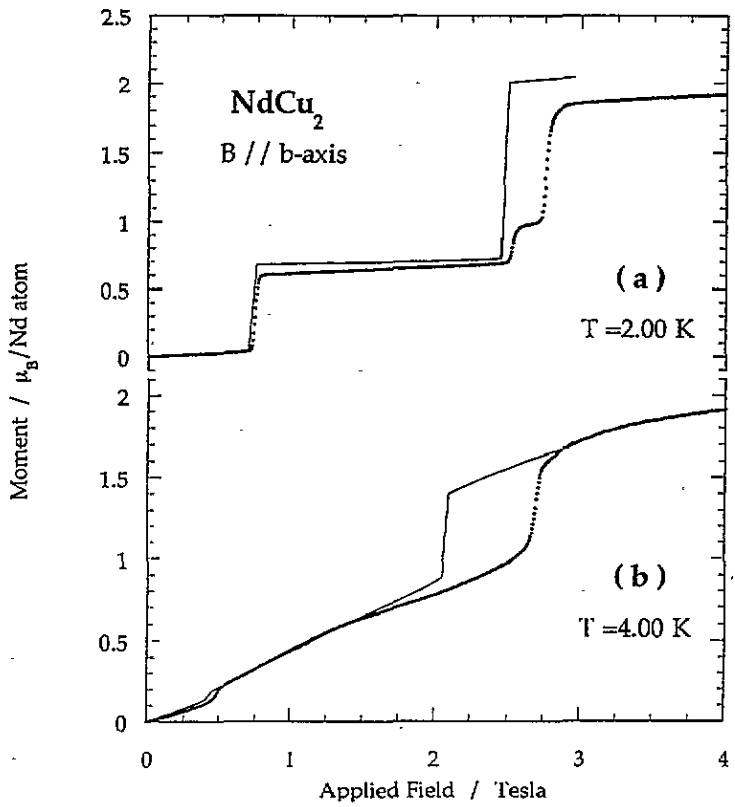

Figure 6. Comparison of isothermal magnetization measurements made at (a) 2.0 K and (b) 4.0 K (symbols) with the model calculations (solid line).

These occur in the region marked INC. The model also predicts a phase (marked F2 in figure 7(b)), consisting of 16 *b*–*c* planes. However, we have not found any experimental evidence in the magnetization measurements that support the existence of this phase in that region of the magnetic phase diagram determined by the model.

5. Conclusion

Based on detailed magnetization measurements on a single crystal, a magnetic phase diagram of $NdCu_2$ has been constructed. This contains some modifications with respect to previously published phase diagrams. In combination with neutron diffraction experiments, the spin structure of the various phases in the diagram has been derived. The discussion of the various spin arrangements is accompanied by a model calculation using mean-field theory. There is good qualitative agreement between the calculation and the experimental results obtained from magnetization and neutron diffraction. Improving the quantitative agreement mainly at higher temperature and higher fields needs to go beyond the mean-field theory. Magnetostriction experiments [10], which will be extended below 1.6 K in the near future, may help to clarify open questions with respect to the F1 → F3 transition.

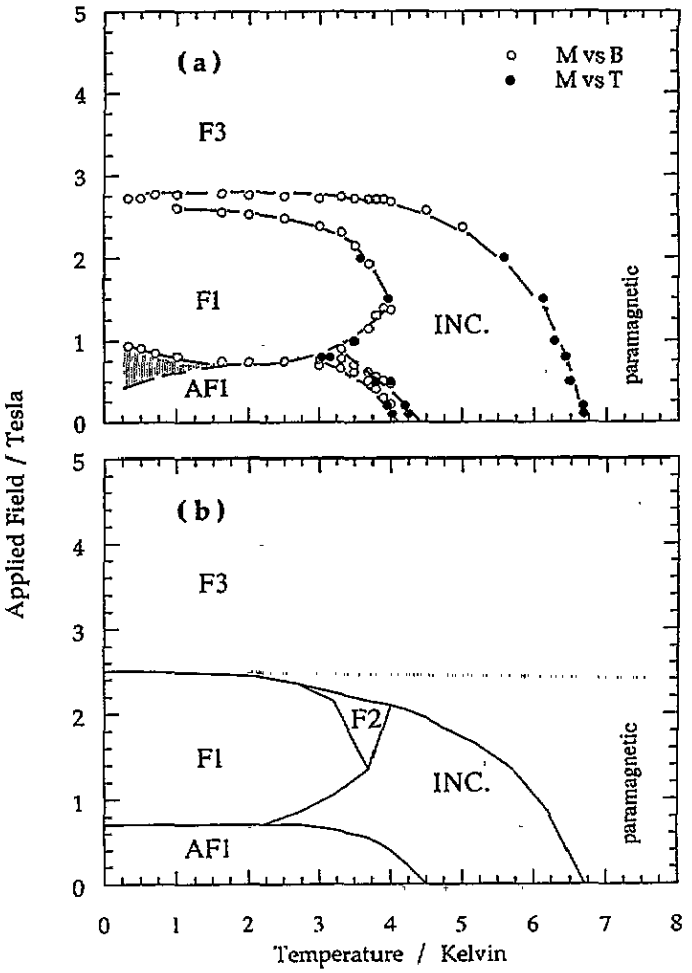

Figure 7. (a) The magnetic phase diagram constructed from magnetization data taken in a constant field (•) and at constant temperature (○). The dashed lines serve as a guide for the eyes. (b) The magnetic phase diagram as obtained from the model calculation.

Acknowledgments

We thank M Loewenhaupt for stimulating discussions. Parts of the work were supported by the 'Austrian Science Foundation' under project No 9203. MR is indebted to the 'Österreichische Forschungsgemeinschaft' for financial support. ME, MdP and KAM acknowledge support from the UK Science and Engineering Research Council and the Wolfson Foundation.

References

[1] Gratz E, Loewenhaupt M, Divis M, Steiner W, Bauer E, Pillmayr N, Müller H, Nowotny H and Frick B 1991 *J. Phys.: Condens. Matter* **3** 9297

[2] Bozukov L, Gilewski A, Gratz E, Apostolov A and Kamenov K 1992 *Physica* B **177** 299

[3] Gratz E, Rotter M, Lindbaum A, Müller H, Bauer E and Kirchmayr H 1993 *J. Phys.: Condens. Matter* **5** 567

[4] Svoboda P, Divis M, Andreev A V, Baranov N V, Bartashevich M I and Markin P E 1992 *J. Magn. Magn. Mater.* **104–107** 1329
[5] Arons R R, Loewenhaupt M, Reif Th and Gratz E 1994 *J. Phys.: Condens. Matter* **6** 6789
[6] Loewenhaupt M, Reif Th, Arons R R, Gratz E, Rotter M and Lebech B 1995 *Z. Phys.* B at press
[7] Loewenhaupt M, Reif Th, Gratz E, Rotter M and Lebech B 1995 to be published
[8] Gignoux D, Morin P, Voiron J and Burlet P 1992 *Phys. Rev.* B **46** 8877
[9] Jensen J and Mackintosh A R (ed) 1991 *Rare Earth Magnetism* (Oxford: Clarendon) ch 2
[10] Zochowski S W, Rotter M, Gratz E and McEwen K A 1995 *Proc. ICM'94; J. Magn. Magn. Mater.* at press